Using Local Climate Zone scheme for UHI assessment: Evaluation of the method using mobile measurements

François Leconte, Julien Bouyer, Rémy Claverie, Mathieu Pétrissans

Using Local Climate Zone scheme for UHI assessment: evaluation of the method using mobile measurements

Francois Leconte[a,b,d,*], Julien Bouyer[b], Rémy Claverie[b,c], Mathieu Pétrissans[d]

[a] *ADEME, 20 Avenue du Grésillé, BP 90406, 49004 Angers Cedex 01, France*
[b] *CEREMA Direction Territoriale Est, 71 Rue de la Grande Haie, 54520 Tomblaine, France*
[c] *GEMCEA, 149 rue Gabriel Péri, 54500 Vandoeuvre-les-Nancy, France*
[d] *LERMAB, Boulevard des Aiguillettes, BP 70239, 54506 Vandoeuvre les Nancy Cedex, France*

Abstract

In the context of expansion of cities and raise of climate change awareness, urban planers are looking for methods and tools in order to take into account the urban heat island phenomenon. This study analyzes the way urban fabric modifies urban climate through the utilization of a climate scheme called Local Climate Zone (LCZ). This classification has been applied in Nancy (France). Urban indicators have been calculated so as to build 13 LCZ in the Great Nancy Area. The screen-height air temperature distribution has been investigated inside these LCZ via mobile measurements. Air temperature amplitude has mainly demonstrated lower values at nighttime than in daytime in urbanized LCZ types. Recurrent microscale hotspots and coldspots have been located in LCZ presenting heterogeneous urban fabric. Two Control Sites (CS) have been built in each LCZ. The CS average temperature has revealed good likeness with the spatially averaged air temperature. Average nocturnal air temperature differences between pairs of LCZ types have been obtained. These differences vary from less than 1℃ for close LCZ types to more than 4℃ for dissimilar LCZ types.

Keywords:

*Corresponding author
Email addresses: francois.leconte@cerema.fr (Francois Leconte), julien.bouyer@cerema.fr (Julien Bouyer), remy.claverie@cerema.fr (Rémy Claverie), mathieu.petrissans@univ-lorraine.fr (Mathieu Pétrissans)

Local Climate Zone, Mobile Measurements, Urban Climate, Urban Fabric, Urban Heat Island, Urban Indicators

1. Introduction

According to climate change scenarios, European cities are likely to experience more intense and more frequent heat waves in the twenty first century (Christensen et al., 2007). In urban context, heat waves can have significant implications on public health (Koppe et al., 2004), energy consumption (deMunck et al., 2013) and outdoor thermal comfort (Alexandri and Jones, 2008). Consequently, the integration of future climate variability to urban planning strategies becomes a raising challenge for the next decades (Alcoforado and Matzarakis, 2010) (Grimmond et al., 2010).

Heat waves periods tend to reinforce the Urban Heat Island (UHI) phenomenon (Cantat, 2004) (Tan et al., 2010). The amplitude of the UHI is usually expressed as the synchronous screen-height air temperature difference between urban and rural thermal sensors (Stewart and Oke, 2012). Recognized causes of UHI are the decrease of wind speed, the increase of radiative trapping due to the three-dimensional morphology of the cities, the energy storage in urban materials, the decrease of evapotranspiration in relation to the reduction of vegetalized and pervious surfaces in city centers and the heat release due to human activity (Hidalgo et al., 2008).

In order to investigate the relationships between urban fabric and local climate, scientists have developed different classifications such as the FRAISE ("Flux Ratio-Active Index Surface Exchange") scheme (Loridan and Grimmond, 2012), which defines Urban Zones that characterize Energy partitioning (UZE). UZE classification involves the Surface Energy Balance (SEB) scheme (Oke, 1987) and aims to distinguish urban areas in terms of how they partition incoming total downward radiation (which corresponds to solar radiation and longwave radiation). Since urban environment implies local climate modification, another relevant approach consists in incorporate urban indicators to design a climate classification. Urban Climatic Maps (UCMaps) are based on this approach. They are built using land use information, topographic information and climatic data (see (Ren et al., 2011) for a review). Once produced, these maps provide enhanced climatic understanding of the region of interest and urban planning recommendations.

In the same manner, Urban Climate Zone (UCZ) is a simple urban classification scheme which uses urban descriptors dealing with urban morphology

and land use (Oke, 2004). UCZ scheme classifies urban areas regarding the way they modify the wind, thermal and moisture variables. This work has been extended by Stewart who further introduced Local Climate Zone (LCZ) (Stewart, 2011). A Local Climate Zones is defined as an area with a minimum diameter of 400 m which demonstrates both uniform features in terms of urban morphology, land use, urban material and urban metabolism, and a characteristic screen-height temperature regime under calm and clear sky. (Stewart and Oke, 2012).

One of the major advantages of the LCZ scheme is the possibility to redefine urban heat island magnitude. As Stewart highlighted (Stewart, 2011), the usual UHI definition can be discussed, on the one hand because the use of the adjectives "urban" and "rural" may be misleading, and on the other hand because these adjectives may be too simple to describe the complex layout of cities. Unlike the common definition, the LCZ scheme uses standardized descriptions of urban and rural landscapes and defines the UHI amplitude as the screen-height air temperature difference between two specific LCZ that are significantly different in terms of morphology and land cover. The use of UCZ and LCZ schemes has provided an overview of the air temperature distribution in Glasgow (UK) (Emmanuel and Krüger, 2012), Toulouse (France) (Houet and Pigeon, 2011), Nagano (Japan), Vancouver (Canada) and Uppsala (Sweden) (Stewart et al., 2013). Nocturnal difference of 2.6℃ have been observed in Toulouse between UCZ 2 and UCZ 7 whereas nocturnal difference from 2.8℃ to 5℃ have been recorded between LCZ 2 and LCZ D in Uppsala.

This work aims to apply the LCZ scheme in the Great Nancy Area (France) in order to investigate on what extent a homogeneous urban fabric leads to a specific thermal pattern under calm, clear sky. The air temperature distribution inside LCZ, the relationship between urban indicators and air temperature features, and the air temperature differences between LCZ types are particularly analyzed.

2. Materials and methods

2.1. Site description

Nancy conurbation, which numbers approximately 286,000 inhabitants, is located in the North-East part of France (Lat/Long: 48 41'N - 6 11'E) in the center of the Lorraine plateau. North sea shore is about 400 km North-West, the Jura Mountains are about 200 km South. The general climate type

is Cfb (i.e. temperate, with warm summer, without dry season) according to Köppen-Geiger climate classification (Peel et al., 2007). At mesoclimatic scale, Nancy is in a half-basin situation with two plateaus West and North-East and a plain South and East. The Meurthe river and the Marne-Rhine channel pass in the center of the urban area. July is the warmest month of the year, with an average air temperature between 13.7℃ (minimum) and 25.1℃ (maximum).

2.2. Micrometeorologic mobile survey

Mobile measurement method has been chosen since it allows to probe the spatial air temperature distribution inside LCZ. The mobile survey approach has been widely used in urban climate studies such in Lodz (Poland) (Klysik and Fortuniak, 1999), Szeged (Hungary) (Unger et al., 2001), Utrecht (Netherlands) (Brandsma and Wolters, 2012) or Leipzig (Germany) (Schwarz et al., 2012). This field experiment targets to take advantage of this method, recording screen-height air temperature in numerous streets of a LCZ. Therefore car itineraries have been defined in order to investigate in details each selected LCZ and traverses have been realized both daytime and nighttime during summer 2012 (Leconte et al., 2012) and summer 2013, each time between July and September.

In this context, the topography of the conurbation has been taken into account. Indeed, if a LCZ exhibits significant altitude changes, the itinerary needs to be adapted in order to estimate the influence of topography on the spatial air temperature distribution. A digital elevation map (resolution of 1 m) has been used to identify LCZ exhibiting significant altitude changes.

Measurements have been performed for low nebulosity (0 to 2 octas) and low wind speed (below 9 $m.s^{-1}$, wind speed at 10 m high), in anticyclonic conditions with dry road surface. In most of the case, these meteorological conditions were similar during the previous day. In case of rain, measurements have been postponed from 24 h at least.

One measurement session takes approximately 2 h 30 min. Considering the air temperature evolution that takes place at mesoclimatic scale during one traverse (about 2℃ at nighttime), a linear time-correction scheme has been applied. The air temperature at the beginning of the session is the reference temperature. The scheme consists in correcting the measured air temperature proportionally to the elapsed time between the beginning of the session and the measurement. This scheme offers the possibility to analyze mobile measurements in a synchronous manner.

(a)

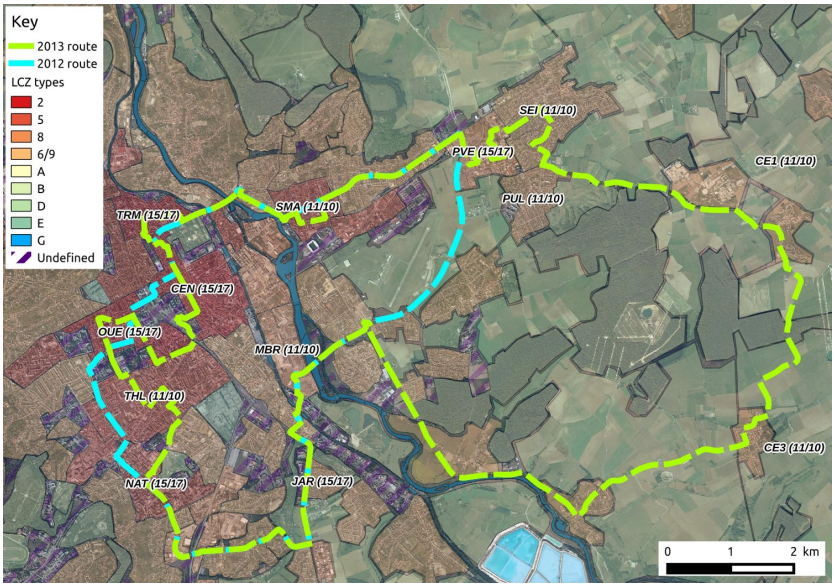

(b)

Figure 1: (a) Map of the Great Nancy Area. Scale 1:55000. (b) LCZ map of the Great Nancy Area. The 13 selected LCZ for the field experiment and the routes performed in 2012 and 2013 are displayed. The number of traverses per LCZ are in parenthesis (number of diurnal traverses/number of nocturnal traverses). Scale 1:55000.

Starting hour for daytime measurements was 2pm (i.e. approximately solar noon), before the theoretical daily maximum air temperature hour, whereas the starting hour for nighttime measurements was 12am (i.e. approximately 3 h after sunset), before the theoretical maximum of UHI amplitude.

Mobile measurements have been completed with an instrumented vehicle. Air temperature at 2 m high have been recorded using a PT 100 probe with an accuracy of ±0.2℃ installed inside a ventilated cylinder mounted on the roof of the car. Measurements have been realized at a 3 m distance step.

During measurement sessions, the instrumented car is embedded in the traffic. Heat release from other vehicles may artificially increase the air temperature recorded and cause a bias in the data. In order to lower this effect, measurements points were excluded from the data set when the car was stopped. Therefore, measurements points in the data set correspond to a car speed between 15 $km.h^{-1}$ and 60 $km.h^{-1}$.

2.3. LCZ building process

The first step of the LCZ building methodology, i.e. metadata gathering, provides a list of ten climatic indicators that are relevant to calculate or estimate, namely:

- Morphological indicators
  - Sky view factor (-)
  - Canyon aspect ratio (-)
  - Mean building height (m)
  - Terrain roughness class (-)
- Land use indicators
  - Building surface fraction (%)
  - Impervious surface fraction (%)
  - Pervious surface fraction (%)
- Urban material indicators
  - Surface admittance ($J.m^{-2}.s^{0.5}.K^{-1}$)
  - Surface albedo (-)

- Anthropogenic indicator
  - Anthropogenic heat flux ($W.m^{-2}$)

Metadata can be collected through field visit, GIS calculations (Houet and Pigeon, 2011) or satellite data (Bechtel and Daneke, 2012) (Gamba et al., 2012). The second step, i.e. source area definition, can be performed using either a footprint model (Schmid, 2002), or a "rule of thumb" approach which suggests that the size of the source area does not extent a few hundreds m (Stewart and Oke, 2012). In (Stewart et al., 2013), source area size is about 100 m radius for densely built area and 200 m radius for open land areas. For the third step, urban indicators calculations are used to choose the most relevant LCZ type amongst the 17 existing LCZ types (10 urbanized, 7 non-urbanized).

In the present study, the LCZ building process for the region of interest has consisted in two steps:

- Firstly, an initial LCZ map has been established considering urban morphology and land use.
- Secondly, LCZ contours have been adjusted by calculating seven urban indicators over ten. Sky view factor has been calculated using SAGA GIS (Böhner et al., 2006) and a Digital Surface Model (DSM) of the region of interest. Aspect ratio has been calculated using the expression proposed in (Masson, 2000). Terrain roughness class has been determined for each LCZ according to the Davenport classification (Davenport et al., 2000). Building surface fractions have obtained from urban GIS database. Impervious and pervious surface fractions have been manually calculated using visible satellite imagery data. Surface albedo, surface admittance and anthropogenic heat flux have not been estimated because of a lack of input data regarding urban materials and anthropic activities.

In addition, two Control Sites (CS) have been selected for each LCZ. The purpose of these CS is to study air temperature differences that can occur inside a LCZ and to provide information about how topoclimatic effects are controlled. A CS is defined as a portion of street, whose length is between 50 m and 100 m, which has been chosen in order to be representative of the overall LCZ surface in terms of urban indicators.

Control Sites have been built according to the following process:

- Within a buffer zone of 100 m around a Control Site, urban indicators values should match with the average urban indicators values of the LCZ.
- A Control Site can not be placed at the edge of the LCZ (minimum distance of 100 m between the Control Site and the border of the LCZ).
- Urban elements which are not representative of the LCZ should be avoided (e.g. squares, fountains).
- Control Site should be located in streets which are representative of the LCZ (e.g. backstreets).
- Crossroads, stops and traffic light should be avoided.
- The distance between two Control Sites of one single LCZ should be maximized.

Urban indicators calculations in the buffer zone of a Control Site adopt the same methodology as calculations at LCZ level, except that the terrain roughness class has not been calculated.

2.4. Post measurements process on air temperature data set

Several post-processing steps have been performed on the air temperature data set in order to produce thermal indicators. The following calculations consider N_p as the number of measurements points recorded over a road section p and $Tair_{p,u}$ the air temperature measured at the point u of the road section p. The air temperature amplitude of the road section p, written as $\Delta Tair_p$, is defined as

$$\Delta Tair_p = max(Tair_p) - min(Tair_p) \tag{1}$$

The spatial mean air temperature over the road section p, written as $\overline{Tair}_p$, is defined as

$$\overline{Tair}_p = \frac{1}{N_p} \sum_{u=1}^{u=N_p} Tair_{p,u} \tag{2}$$

The difference of spatial mean air temperature between LCZ X and LCZ Y for the road section p, written as $\Delta Tair_{p,LCZ\ X-Y}$, is defined as

$$\Delta Tair_{p,LCZ\ X-Y} = \overline{Tair}_p\ in\ LCZ\ X - \overline{Tair}_p\ in\ LCZ\ Y \tag{3}$$

The difference to the spatial mean air temperature at the point u for the road section p, written as $\delta Tair_{p,u}$, is defined as

$$\delta Tair_{p,u} = Tair_{p,u} - \overline{Tair}_p \tag{4}$$

Considering N_{LCZ} as the number of traverses performed for a given LCZ, the average of the difference to the spatial mean air temperature, written as $\overline{\delta Tair_u}$, is defined as

$$\overline{\delta Tair_u} = \frac{1}{N_{LCZ}} \sum_{p=1}^{p=N_{LCZ}} \delta Tair_{p,u} \tag{5}$$

Considering N_{CSx} as the number of measurements points recorded inside a given Control Site CSx over a road section p, the Control Site temperature, written as $Tair_{CSx,p}$, is defined as

$$Tair_{CSx,p} = \frac{1}{N_{CSx}} \sum_{u=1}^{u=N_{CSx}} Tair_{p,u} \tag{6}$$

The difference of temperature between two Control Sites (CS1 and CS2) for the road section p, written as $\Delta Tair_{CS,p}$, is defined as

$$\Delta Tair_{CS,p} = Tair_{CS1,p} - Tair_{CS2,p} \tag{7}$$

The average temperature of two Control Sites for the road section p, written as $\overline{Tair}_{CS,p}$, is defined as

$$\overline{Tair}_{CS,p} = \frac{Tair_{CS1,p} + Tair_{CS2,p}}{2} \tag{8}$$

3. Results

3.1. Indicators calculations and LCZ map of Nancy

LCZ map of the Great Nancy Area (GNA) is presented Figure 1. Due to the specific urban features of the Great Nancy Area, only 10 types of LCZ (over the 17 existing types of LCZ) have been used. Thirteen LCZ of different types have been selected for the field experiment. The chosen locations vary

from downtown Nancy to the periphery of the region of interest. Urban indicators values are presented from Figure 2 to Figure 6.

Several residential areas, namely JAR, SEI and PUL, are on the edge between type 6 and type 9 in terms of land use fractions (Figure 4). Morphological indicators values do not allow to determinate a LCZ type, since sky view factor values are type 6 and aspect ratio values are type 9. In this ambiguous situation, any choice has been performed. Consequently these three LCZ are considered as type 6/9. In the case of MBR and PVE (Figure 5), land use indicators do not exactly match with type 8 values. However, the text definition and illustrations of the LCZ type 8 clearly argue for identifying these two LCZ as a type 8. Thus MBR and PVE have been considered as LCZ type 8. In non-urbanized LCZ (CE1 and CE3, Figure 6), sky view factor has not been calculated because the required satellite data was not available. Nevertheless, field visits indicate that the sky view factor values for these LCZ are very likely to be into the accurate range of values.

Except the three equivocal LCZ type 6/9, urban indicators calculated both at LCZ level and at Control Site level generally fall into the suggested range of values for the corresponding type of LCZ. Indicators that are out of the suggested range of values are reasonably close. The maximum distance between calculated values and suggested values is 0.07 for sky view factor, 0.07 for aspect ratio, and 7% land use fractions. This result confirms that the selected LCZ building process is suitable for this study, since existing urban areas have been identified to LCZ type with acceptable mismatch.

Besides, urban indicators values calculated inside of the Control Sites buffer zone are generally close to urban indicators values for the global LCZ. A few gaps between CS values and LCZ values are observed for the sky view factor indicator. This comes from slight differences in sky view factor calculation method between Control Site (street canyon sky view factor) and LCZ (area-averaged sky view factor). Overall, it seems that Control Sites locations have been chosen appropriately in terms of urban indicators representativeness.

At the end of the LCZ building process, the sum of all LCZ surface does not cover all the region of interest. The reason is that several areas do not meet the LCZ scheme requirements, either because their diameter is smaller than 400 m, or because they present important inhomogeneities in surface structure, cover, fabric and metabolism in a way that they can not be identified to a specific LCZ type (hatched areas in Figure 1(b)).

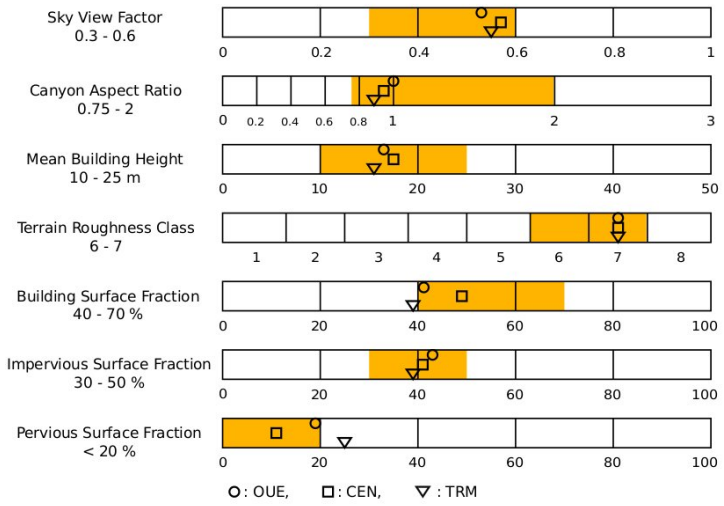

(a)

(b)

(c)

Figure 2: (a) Indicators range for a LCZ type 2 Compact Midrise. Indicators values for OUE, CEN, TRM. (b) Street view in OUE (e) Airborne view of OUE. Scale 1:5000.

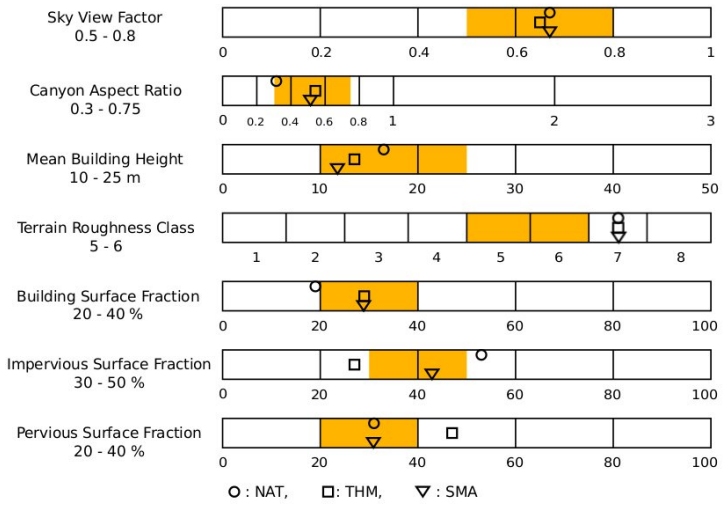

(a)

(b)

(c)

Figure 3: (a) Indicators range for a LCZ type 5 Open Midrise. Indicators values for NAT, THM, SMA. (b) Street view in SMA (e) Airborne view of SMA. Scale 1:5000.

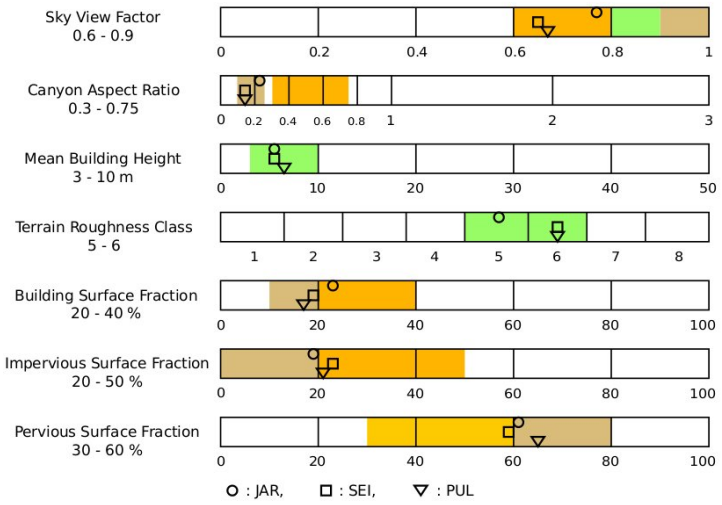

(a)

(b)

(c)

Figure 4: (a) Indicators range for a LCZ type 6 Open Lowrise in orange. Indicators range for a LCZ type 9 Sparsely Built in brown. Range of values that are both in LCZ type 6 and LCZ type 9 are in green. Indicators values for JAR, SEI, PUL. (b) Street view in SEI (e) Airborne view of SEI. Scale 1:5000.

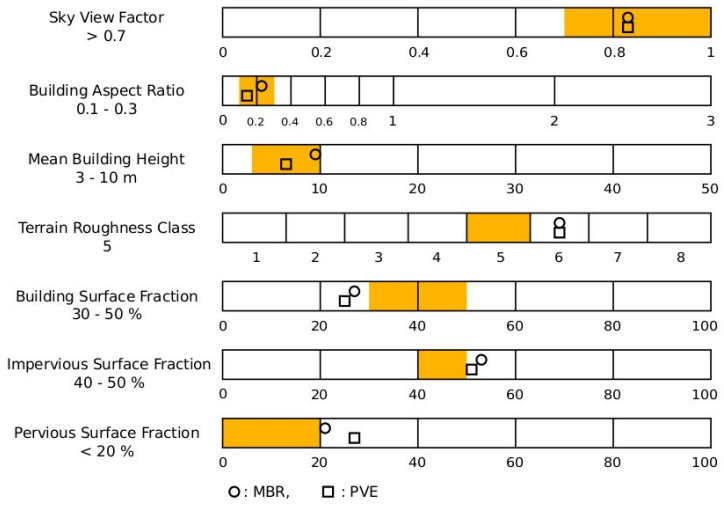

(a)

(b)

(c)

Figure 5: (a) Indicators range for a LCZ type 8 Large Lowrise. Indicators values for MBR, PVE. (b) Street view in PVE (e) Airborne view of PVE. Scale 1:5000.

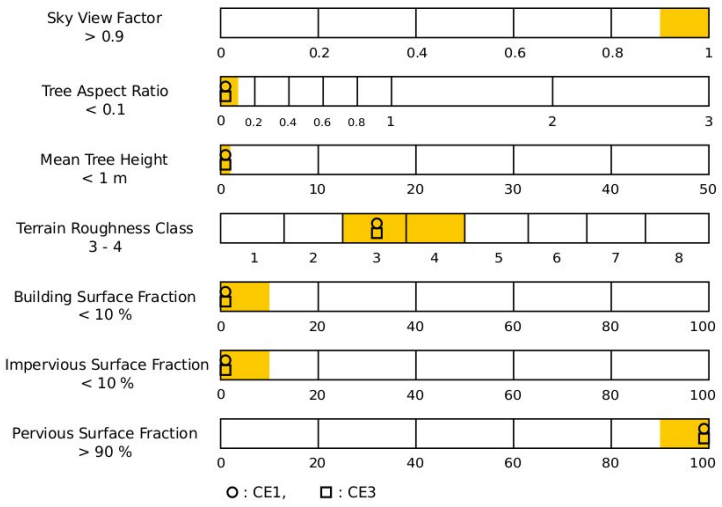

(a)

(b)

(c)

Figure 6: (a) Indicators range for a LCZ type D Low Plants. Indicators values for CE1, CE3. (b) Street view in CE3 (e) Airborne view of CE3. Scale 1:5000.

3.2. Mobile measurements outcome: spatial variability of air temperature inside LCZ

3.2.1. Air temperature amplitude inside LCZ

The air temperature amplitude $\Delta Tair_p$ in the 13 selected LCZ is presented in Figure 7. During daytime, air temperature amplitude in LCZ type 2 and 5 tend to be higher than in LCZ type 8, 6/9 and D (Figure 7(a)). In LCZ type 2 and 5, amplitude values are scattered over 2℃ while in LCZ type 8, 6/9 and D amplitude values are more often comprised within 1℃.

Unlike the other LCZ types used in the Great Nancy Area, LCZ type 2 and 5 exhibit specific values of morphological indicators. Sky view factor is always below 0.7, aspect ratio is above 0.35, mean building height is above 10 m and terrain roughness class is 7. These particular morphological features may explain the observed air temperature amplitude distribution. Due to urban morphology and street orientation, daytime total direct solar radiation that reaches urban materials varies from one street to another. This difference in terms of incoming radiations between streets can lead to a more heterogeneous air temperature distribution within LCZ type 2 and 5.

In addition, anthropogenic flux may be more important in LCZ type 2 and 5 during daytime, which may lead to a positive air temperature anomaly (called hotspot). Conversely, vegetated areas located in dense and urbanized LCZ types could imply a negative air temperature anomaly (called coldspot) due to significant evapotranspiration in daytime. Both phenomenons may lead to a greater daytime air temperature amplitude inside LCZ.

Except for SEI and LCZ type D, air temperature amplitude is mainly between 0.5℃ and 2℃ during nighttime (Figure 7(b)). Air temperature amplitude in LCZ type 2 and 5 as well as in JAR tend to be lower in nighttime than in daytime, whereas air temperature amplitude in LCZ type 8, PUL and CE3 seems to be similar between the two periods. The general trend shows that in all urbanized types of LCZ, air temperature distribution tends to be more homogeneous in nighttime, i.e. with a lower air temperature amplitude. Greater nocturnal air temperature amplitude in SEI is very likely due to cold air advection from a contiguous LCZ type D. Greater nocturnal air temperature amplitude in CE1 is probably driven by a topoclimatic effect. Indeed, a low point (i.e. an altitude drop of 14 m over a portion of road of 600 m) tends to lead to an air temperature drop.

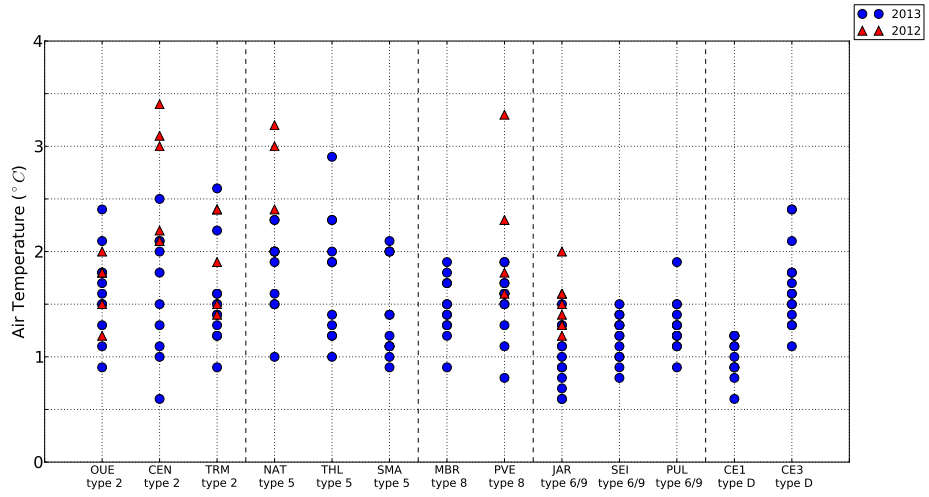

(a)

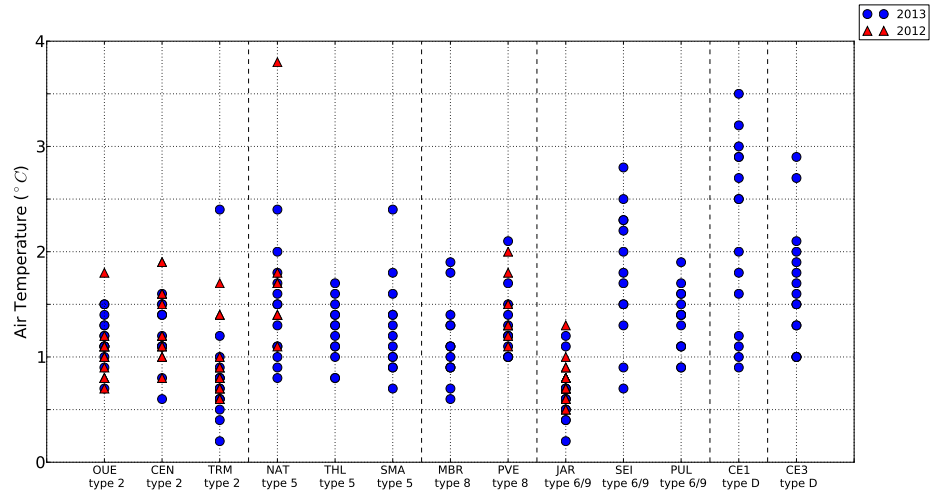

(b)

Figure 7: Air temperature amplitude $\Delta Tair_p$ inside the 13 selected LCZ, sorted by LCZ type. Red triangles correspond to traverses performed in 2012. Blue circles correspond to traverses performed in 2013. (a) Diurnal period. (b) Nocturnal period.

3.2.2. Recurrent hotspots and coldspots inside LCZ

Figure 8 aims to locate hotspots and coldspots within JAR and NAT, presenting the average over 11 traverses of the difference to the spatial mean air temperature $\overline{\delta Tair_u}$. JAR does not reveal recurrent climate inhomogeneities, neither daytime nor nighttime, since the dispersion of $\overline{\delta Tair_u}$ is tight (between -0.2℃ and 0.2℃). Conversely, NAT offers a greater dispersion of $\overline{\delta Tair_u}$ (between -0.6℃ and 0.4℃ in daytime, between -0.9℃ and 0.5℃ in nighttime). In this latter LCZ, a few areas are recurrent hotspots and coldspots relatively to the spatial mean air temperature. These climatic inhomogeneities should be related to peculiarities in terms of urban features. For instance in Figure 8(d), the nocturnal coldspot (dark blue area south of the LCZ) is a tree-planted avenue while the nocturnal hotspot (bright red area in the middle of the LCZ) is localized in an impervious environment. In general, small LCZ with homogeneous urban morphology and indicators (e.g. JAR) have less hotspots and coldspots than large LCZ with heterogeneous urban morphology (e.g. NAT).

Another noticeable element is that nocturnal hotspots and coldspots do not systematically match with diurnal hotspots and coldspots. This result highlights that the thermal difference to the spatial mean air temperature evolves considerably throughout the time at microscale, under the influence of numerous parameters such as street orientation, local winds and anthropogenic heat release.

3.2.3. Thermal behavior of Control Sites

Results show that air temperature differences between two Control Sites of one given LCZ are acceptable. 96% of the $\Delta Tair_{CS,p}$ values are between -1℃ and 1℃, and 74% are between -0.5℃ and 0.5℃. This fact illustrates that in general topoclimatic effect seems to have been controlled and that Control Site have been accurately chosen.

The difference between the spatial mean air temperature $\overline{Tair}_p$ and the arithmetical average of the two Control Sites $\overline{Tair}_{CS,p}$ is presented Figure 9. Except two traverses in PVE and NAT, the difference between these two indicators is equal or below 0.5℃ both daytime and nighttime. $\overline{Tair}_p$ and $\overline{Tair}_{CS,p}$ are very close, i.e. the arithmetical average of the Control Sites represents fairly well the spatially averaged air temperature of an LCZ.

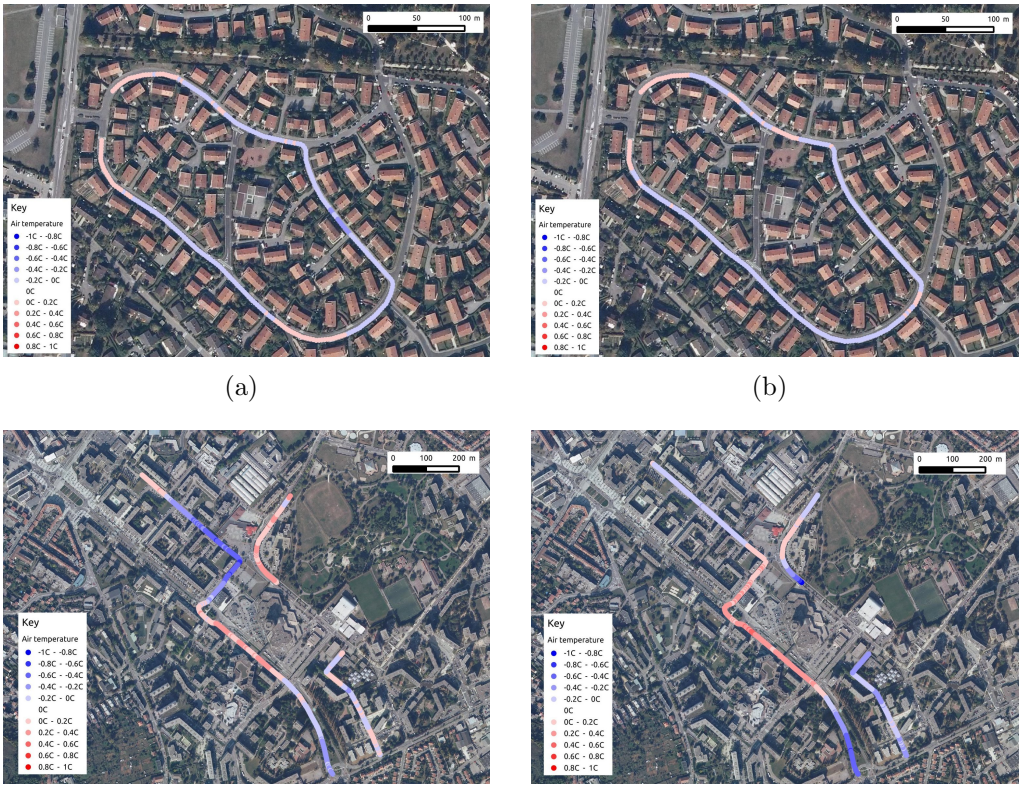

(a) (b)

(c) (d)

Figure 8: Average over 11 traverses of the difference to the spatial mean air temperature $\overline{\delta Tair_u}$. (a) Diurnal period in JAR. (b) Nocturnal period in JAR. (c) Diurnal period in NAT. (d) Nocturnal period in NAT.

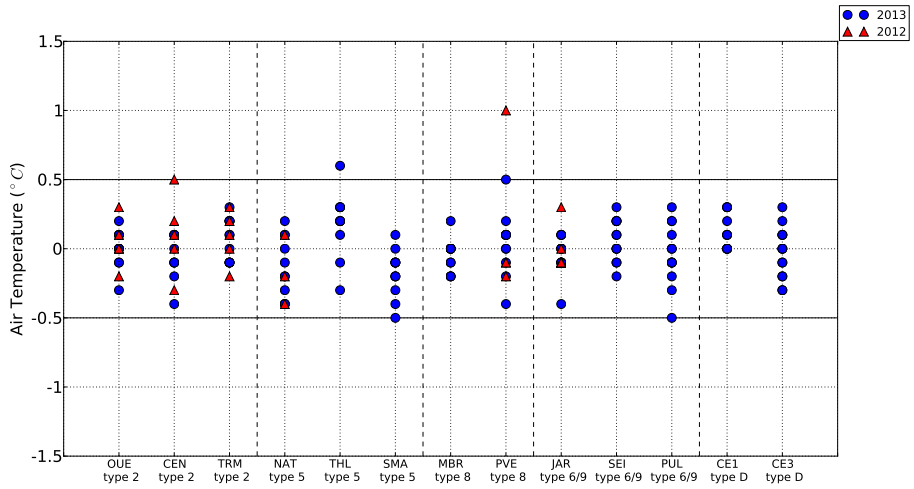

(a)

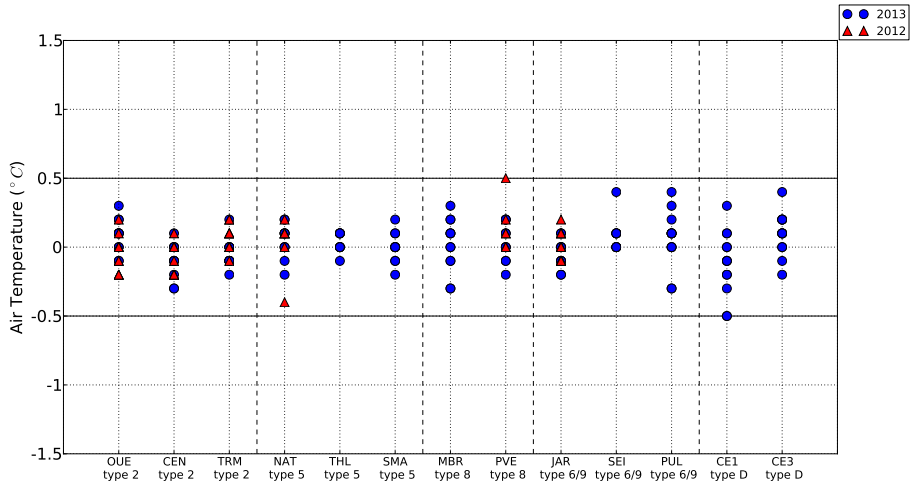

(b)

Figure 9: Difference between $\overline{Tair}_{CS,p}$ and $\overline{Tair}_p$ ($\overline{Tair}_{CS,p}$ - $\overline{Tair}_p$), sorted by LCZ type. Red triangles correspond to traverses performed in 2012. Blue circles correspond to traverses performed in 2013. (a) Diurnal period. (b) Nocturnal period.

3.3. Synchronous mean air temperature comparison between LCZ

Table 1 presents the summary of the synchronous mean air temperature $\Delta Tair_{LCZ\ X-Y}$, both daytime and nighttime. At daytime, all $\Delta Tair_{LCZ\ X-Y}$ are below 1℃. LCZ types 2 and 8 are the hottest LCZ type while LCZ type D seems to be the coldest LCZ type. These experimental results correspond to the literature, which states that the urban heat island amplitude is limited at mid-afternoon. At nighttime, LCZ types may be separated into three groups, namely LCZ types 2 and 5 (group 1), LCZ types 8 and 6/9 (group 2) and LCD type D (group 3). Average air temperature difference between group 1 and group 2 is from 1.3℃ to 1.8℃ while average air temperature difference between group 1 and group 3 is from 4.2℃ to 4.4℃. Similarly to daytime, LCZ type 2 is the hottest LCZ type while LCZ type D is the coldest LCZ type.

The characteristics of the LCZ types provide explanations about these nocturnal temperature difference between LCZ. Indeed, considering the indicators values for the studied LCZ, common features can be found within each group. As introduced in section 3.2.1, similar pattern for morphological indicators can be found for group 1. It is also the case for LCZ group 2, which shows different values from group 1: sky view factor is always above 0.6, aspect ratio is below 0.2, mean building height is below 10 m and terrain roughness class is 6 or below. Regarding land use, values from group 1 are scattered whereas it is possible to notice that building surface fraction is always below 30% within group 2. Another important point is that the studied LCZ of group 1 are located in the geographical center of the urban area while LCZ of group 2 are mostly located in the periphery of the city. Group 3, i.e. LCZ type D, is significantly different than the other LCZ types studied, with low height vegetation and without any buildings.

4. Discussion

The LCZ building process performed in the Great Nancy Area have risen several challenges. Since the region of interest is a continuously urbanized territory, the determination of the LCZ contours have not been always straightforward. While some LCZ are very homogeneous in terms of urban indicators (JAR), some others are more heterogeneous (NAT), with important local variations of urban indicators. Local knowledge of the urban fabric have been required at this step. Besides, LCZ map of Nancy shows that many LCZ have a diameter slightly above 400 m. LCZ with large diameter,

LCZ Type	2	5	6/9	8	D
2	-	0.2 (0.5)	1.8 (0.6)	1.5 (0.6)	4.4 (1.0)
5	0.4 (0.3)	-	1.5 (0.6)	1.3 (0.7)	4.2 (1.0)
6/9	0.3 (0.3)	-0.1 (0.4)	-	-0.3 (0.4)	2.4 (0.7)
8	0.0 (0.3)	-0.3 (0.3)	-0.2 (0.3)	-	2.9 (0.7)
D	0.8 (0.5)	0.5 (0.4)	0.6 (0.4)	0.8 (0.4)	-

Table 1: Average difference between pairs of LCZ types $\Delta Tair_{LCZ\ X-Y}$. Bottom left area is the difference between the LCZ type in column minus the LCZ type in row and corresponds to the daytime period. Upper right area is the difference between the LCZ type in row minus the LCZ type in column and corresponds to the nighttime period. Standard deviation are in parenthesis.

i.e. above 1000 m, are rare. This constellation of small LCZ is due to the medium size of the conurbation as well as the history of urban development of the city.

Quality and availability of input data are crucial for the indicators calculation process. Up-to-date satellite maps as well as appropriate GIS algorithms have been key elements. This study has demonstrated the possibility to build LCZ using 7 indicators over 10. Unfortunately, the calculation of the surface albedo, surface admittance and anthropogenic heat flux have not been realized. However, these three urban indicators are not distinct for the urbanized LCZ types used in this study. For instance, range of values for the surface albedo is identical for the LCZ types 5, 6 and 9. Therefore it is impossible to know if their calculation would have lead to a more accurate LCZ identification process in the present case.

This work also highlights that the average air temperature difference between pairs of LCZ types can exhibit values of the same order of magnitude than the air temperature amplitude inside LCZ. Indeed, the air temperature amplitude $\Delta Tair_p$ inside LCZ is sometimes about 2℃ at nighttime, and in the meantime, nocturnal average $\Delta Tair_{LCZ\ 2-6/9}$ is 1.8℃. This result demonstrates that air temperature anomalies at microscale may be significant in comparison to the local scale thermal pattern. As presented section 3.2.2, the study of recurrent hotspots and coldspots inside LCZ can be particularly relevant to locate these inhomogeneities.

The accuracy of the sensor and the measured diurnal values of $\Delta Tair_{LCZ\ X-Y}$ between close LCZ types (Table 1) exhibit the same order of magnitude. However, experimental conditions encountered in this study do not

	Stewart's observations	GNA values
Small difference in morphology and fabric	< 2℃	0.2℃ to 0.5℃
Large difference either in morphology or fabric	2℃ to 5℃	1.3℃ to 1.8℃
Large difference in morphology and fabric	> 5℃	4.2℃ to 4.4℃

Table 2: Nocturnal average difference between pairs of LCZ types measured in the Great Nancy Area compared to Stewart's observations (Stewart, 2011).

allow to use a more accurate technology. Thus, daytime measurements performed in this study can only demonstrate that $\Delta Tair_{LCZ\ X-Y}$ between close LCZ types are below 1℃.

Measured nocturnal values of $\Delta Tair_{LCZ\ X-Y}$ in the Great Nancy Area are compared with Stewart's observations in Table 2. In both cases, a small (resp. large) difference in morphology and fabric corresponds to a small (resp. large) air temperature difference. The range of values obtained in the present study are slightly lower than Stewart proposed. This could be explained by the size of Nancy, which is a relatively small comparing to cities like Vancouver or Nagano. However, nocturnal $\Delta Tair_{LCZ\ X-Y}$ values in Nancy are similar to the values recorded in Uppsala (Stewart et al., 2013), which is also an European middle-size city.

5. Conclusion

This paper aims to contribute to deepen knowledge about air temperature features within LCZ and between pairs of LCZ. To that purpose:

- LCZ scheme has been applied in the Great Nancy Area and a LCZ map has been built. Indicators calculations have allowed to identify existing urban areas to specific types of LCZ.

- Spatial air temperature distribution have been investigated inside LCZ. At nighttime, air temperature amplitude is generally between 0.5 ℃ and 2 ℃ in urbanized LCZ types. Within the LCZ, Control Sites average temperature $\overline{Tair}_{CS,p}$ has demonstrated good similarities with the spatially averaged air temperature.

- Observed microscale thermal inhomogeneities illustrate the existing relationships between urban district layout and screen-height air temperature behavior. Recurrent hotspots and coldspots have been located in LCZ which present heterogeneous urban fabric.

- This relationship is also noticeable at mesoclimatic scale through mean air temperature comparisons between LCZ types. Values of $\Delta Tair_{LCZ\ X-Y}$ range between less than 1℃ for close LCZ types to 4.4℃ for dissimilar LCZ types.

Concerning the experimental approach, mobile surveys have recorded LCZ climate features and have provided high density data. Results indicate that the determination of hotspots and coldspots and the study of climate inhomogeneities in LCZ requires high spatial density data that mobile survey can provide.

Initially, LCZ scheme was built notably to guide UHI studies and improve results communication amongst urban climate researchers. However, this scheme can also be adopted in order to set up a meteorological network over a conurbation, placing meteorological stations within LCZ of interest. In this context, the mobile measurements approach can be relevant since it allows to propose stations sites (e.g. control sites) and to locate non-representative sites (hotspot and coldspot). Furthermore, this simple and intuitive scheme, which has been designed for urban climate observations, could provide a valuable asset to urban planning strategies. Indeed, a comprehensive LCZ map could locate areas that are potentially warmer than others during calm and clear nights in summertime. These specific urban areas could be elected to implement countermeasures to urban heat island.

Aknowledgments

This work has been supported by the French Environment and Energy Management Agency (ADEME) and the GEMCEA.

References

Alcoforado, M., Matzarakis, A., 2010. Planning with urban climate in different climatic zones. Geographicalia 57, 5–39.

Alexandri, E., Jones, P., 2008. Temperature decreases in an urban canyon due to green walls and green roofs in diverse climates. Building and Environment 43, 480–493.

Bechtel, B., Daneke, C., 2012. Classification of local climate zones based on multiple earth observation data. IEEE Journal of Selected Topics in Applied Earth Observations and Remote Sensing 5, 1191–1202.

Böhner, J., McCloy, K., Strobl, J., 2006. SAGA - Analysis and Modeling Applications. Vol. 115.

Brandsma, T., Wolters, D., 2012. Measurement and statistical modeling of the urban heat island of the city of utrecht (the netherlands). Journal of Applied Meteorology and Climatology 51, 1046–1060.

Cantat, O., 2004. L'îlot de chaleur urbain parisien selon les types de temps. Norois 191.

Christensen, J., Hewitson, B., Busuioc, A., Chen, A., Gao, X., Held, I., Jones, R., Kolli, R., Kwon, W.-T., Laprise, R., Magaña Rueda, V., Mearns, L., Menéndez, C., Räisänen, J., Rinke, A., Sarr, A., Whetton, P., 2007. 2007: Regional climate projection. Tech. rep., Climate Change 2007: The Physical Science Basis. Contribution of Working Group I to the Fourth Assessment Report of the Intergovernmental Panel on Climate Change [Solomon, S., D. Qin, M. Manning, Z. Chen, M. Marquis, K.B. Averyt, M. Tignor and H.L. Miller (eds.)]. Cambridge University Press, Cambridge, United Kingdom and New York, NY, USA.

Davenport, A., Grimmond, C., Oke, T., Wieringa, J., 2000. Estimating the roughness of cities and sheltered country. In: 12th Conference of Applied Climatology.

deMunck, C., Pigeon, G., Masson, V., Meunier, F., Bousquet, P., Tréméac, B., Merchat, M., Poeuf, P., Marchadier, C., 2013. How much can air conditioning increase air temperatures for a city like paris, france? International Journal of Climatology 33, 210–227.

Emmanuel, R., Krüger, E., 2012. Urban heat island and its impact on climate change resilience in a shrinking city: The case of glasgow, uk. Building and Environment 53, 137–149.

Gamba, P., Lisini, G., Liu, P., Du, P., Lin, H., 2012. Urban climate zone detection and discrimination using object-based analysis of vhr scenes. In: Proceedings of the 4th GEOBIA.

Grimmond, C., Roth, M., Oke, T., Au, Y., Best, M., Betts, R., Carmichael, G., Cleugh, H., Dabberdt, W., Emmanuel, R., Freitas, E., Fortuniak, K., Hanna, S., Klein, P., Kalkstein, L., Liu, C., Nickson, A., Pearlmutter, D., Sailor, D., Voogt, J., 2010. Climate and more sustainable cities: climate information for improved planning and management of cities (producers/capabilities perspective). Procedia Environmental Sciences 1, 247–274.

Hidalgo, J., Masson, V., Baklanov, A., Pigeon, G., Gimeno, L., 2008. Advances in urban climate modeling. Trends and Directions in Climate Research 1146, 354–374.

Houet, T., Pigeon, G., 2011. Mapping urban climate zone and quantifying climate behaviours - an application on toulouse urban area (france). Environmental Pollution 159, 2180–2192.

Klysik, K., Fortuniak, K., 1999. Temporal and spatial characteristics of the urban heat island of lodz, poland. Atmospheric Environment 33, 3885–3895.

Koppe, C., Kovats, S., Jendritzky, G., Menne, B., 2004. Heat-waves: risks and responses. health and global environmental change. series, no. 2. Tech. rep., World Health Organization.

Leconte, F., Bouyer, J., Claverie, R., Pétrissans, M., 2012. Methodology for semi-empirical climatic modelling using on-board measurements. In: 8th International Conference on Urban Climate.

Loridan, T., Grimmond, C., 2012. Characterisation of energy flux partitioning in urban environments: links with surface seasonal properties. Journal of Applied Meteorology and Climatology 51, 219–241.

Masson, V., 2000. A physically-based scheme for the urban energy budget in atmospheric models. Boundary-Layer Meteorology 94, 357–397.

Oke, T., 1987. Boundary Layer Climate, 2nd Edition. Routledge.

Oke, T., 2004. Initial guidance to obtain representative meteorological observations at urban sites. Tech. Rep. 81, World Meteorological Organization.

Peel, M., Finlayson, B., McMahon, T., 2007. Updated world map of the köppen-geiger climate classification. Hydrology and Earth System Sciences 11, 1633–1644.

Ren, C., Ng, E., Katzschner, L., 2011. Urban climatic map studies: a review. International Journal of Climatology 31, 2213–2233.

Schmid, H., 2002. Footprint modeling for vegetative atmosphere exchange studies: a review and perspective. Agricultural and Forest Meteorology 113, 159–183.

Schwarz, N., Schlink, U., Frank, U., Grossmann, K., 2012. Relationship of land surface and air temperature and its implication for quantifying urban heat island indicators - an application for the city of leipzig (germany). Ecological Indicators 18, 693–704.

Stewart, I., 2011. Redefining the urban heat island. Ph.D. thesis, The University of British Columbia, Vancouver.

Stewart, I., Oke, T., 2012. Local climate zones for urban temperature studies. Bulletin of American Meteorology Society 93, 1879–1900.

Stewart, I., Oke, T., Krayenhoff, E., 2013. Evaluation of the 'local climate zone' scheme using temperature observations and model simulations. International Journal of Climatology (DOI: 10.1002/joc.3746).

Tan, J., Zheng, Y., Tang, X., Guo, C., Li, L., Song, G., X., Z., Yuan, D., Kalkstein, A., Li, F., Chen, H., 2010. The urban heat island and its impact on heat waves and human health in shanghai. International Journal of Biometeorology 54, 75–84.

Unger, J., Sümeghy, Z., Zoboki, J., 2001. Temperature cross-section features in an urban area. Atmospheric Research 58, 117–127.